東北大学機関リポジトリ
TOUR
Tohoku University Repository

Angular distribution of Auger electrons from fixed-in-space and rotating C 1s 2 photoexcited CO: Theory

Angular distribution of Auger electrons from fixed-in-space and rotating C $1s \rightarrow 2\pi$ photoexcited CO: Theory

R. F. Fink,[1,a)] M. N. Piancastelli,[2] A. N. Grum-Grzhimailo,[3,4] and K. Ueda[4]

[1]*Institute of Organic Chemistry, University of Würzburg, D-97074 Würzburg, Germany*
[2]*Department of Physics and Material Science, Uppsala University, P.O. Box 530,*
SE-751 21 Uppsala, Sweden
[3]*Skobeltsyn Institute of Nuclear Physics, Lomonosov Moscow State University, Moscow 119991, Russia*
[4]*Institute of Multidisciplinary Research for Advanced Materials, Tohoku University,*
Sendai 980-8577, Japan

The one-center approach for molecular Auger decay is applied to predict the angular distribution of Auger electrons from rotating and fixed-in-space molecules. For that purpose, phase shifts between the Auger decay amplitudes have been incorporated in the atomic model. The approach is applied to the resonant Auger decay of the photoexcited C $1s \rightarrow 2\pi$ resonance in carbon monoxide. It is discussed how the symmetry of the final ionic state is related to features in the angular distributions and a parametrization for the molecular frame Auger electron angular distribution is suggested. The angular distribution of Auger electrons after partial orientation of the molecule by the $\sigma \rightarrow \pi$-excitation process is also calculated and compared to available experimental and theoretical data. The results of the one-center approach are at least of the same quality as the available theoretical data even though the latter stem from a much more sophisticated method. As the one-center approximation can be applied with low computational demand even to extended systems, the present approach opens a way to describe the angular distribution of Auger electrons in a wide variety of applications. © *2009 American Institute of Physics.* [DOI: 10.1063/1.3042153]

I. INTRODUCTION

Auger electron spectroscopy is a standard tool in the investigation of surfaces and a fundamentally important method for research of the electronic structure of matter. One of the most demanding open questions in molecular Auger spectroscopy is to understand the angular distribution of Auger electrons. There is a particular deficiency in the field of surface Auger spectroscopy, where only those Auger electrons can be investigated, which are emitted toward the detection system and away from the surface. Thus, it is very important to understand the angular distributions of Auger electrons for the physics of condensed matter and surfaces samples. This has been early recognized and applied to determine geometries of adsorbates on surfaces[1] and is still of major importance for surface electron spectroscopy (see Ref. 2 for a recent review on surface Auger electron spectroscopy that mentions this point).

Studies with free molecules remove the solid state effects and give a deeper insight into the dynamics of the molecular Auger decay itself. Measurement of the angular distribution of Auger electrons for molecules in the gas phase, which are partially oriented due to the excitation process, is now a routine task (see, e.g., Refs. 3–5). Much more detailed information can be obtained from the angular distributions of Auger electrons from "fixed-in-space" molecules in the gas phase. Here the molecular axis orientation at the moment of

creating the hole is defined by the direction of an energetic molecular fragment (recoil ion), which is detected in coincidence with the Auger electron.[6,7] This new level of sophistication calls for a deeper theoretical analysis and the development of generally applicable theoretical methods that provide the angular distribution of Auger electrons from molecules, including fixed-in-space molecules.

Theoretical approaches describing the angular distribution of the Auger electrons from molecules[8–20] have been worked out within the two-step approximation, which treats the hole formation and the Auger decay independently.[21–23] In the set of papers in Refs. 12–17 it was shown that (i) the angular distributions of Auger electrons from rotating molecules of arbitrary symmetry, (ii) the spatial orientation of molecular ions after the Auger decay, and (iii) angular correlations between the direction of the Auger emission and the molecular ion orientation can be treated within the same general framework. Their formalism—recently summarized in Ref. 24—explicitly takes into account possible coherences between states of the decaying molecule. The key parameters of this theory are the "anisotropy parameters," expressed in terms of Auger decay amplitudes, and the "order parameters,"[25] describing the anisotropy of the molecular ensemble before the Auger decay. The latter depends on the symmetry of the molecule and on the dynamics of its excitation. In the simplest case of photoinduced resonant Auger decay of a linear molecule in an initially unpolarized Σ state, the order parameters can be found explicitly without dynamic calculations.[16] For the resonant Auger decay of such a molecule, within the two-step approximation, the anisotropy

a)Electronic mail: fink@chemie.uni-wuerzburg.de. Also at Department of Physics and Material Science, Uppsala University, P.O. Box 530, SE-751 21 Uppsala, Sweden.

parameters are the only dynamic quantities to describe the angular distribution of Auger electrons for both fixed-in-space and rotating molecules. Therefore, this case is ideal for analyzing the influence of the dynamics of Auger decay on the angular distribution of Auger electrons.

In a recent work on the resonant Auger decay of the core to the Rydberg excited water molecule, Hjelte *et al.*[26] applied the more advanced one step model to represent the angular distribution of Auger electrons. This work provides indications that the one step model is required in this particular case, where the direct photoionization channel is of similar intensity as the Auger channel. However, the requirement to represent the one step model in both the vibrational and the continuum channel part of the theoretical simulation is very demanding. Thus, it was not possible to reproduce the experimental spectrum with an accuracy that allowed definitive conclusions on this point.

Numerous methods have been used in calculations of molecular Auger decay amplitudes. The first approach was the one-center approximation,[27,28] which has been widely applied to describe normal[29–34] and resonant[35–38] Auger electron spectra of the *KVV*-type. It was also successfully applied to $L_{2,3}VV$ Auger spectra[37,39–41] where it was shown to provide interesting insight into the strong orientational preferences of this electronic process.[42–47] Numerous authors applied scattering methods[10,26,48–55] or the Stieltjes imaging technique.[56–59] Furthermore, several approaches exist that estimate Auger transition rates from population analyses.[60–65] There are much less publications, where the decay amplitudes are applied to obtain the angular distribution of Auger electrons.[10,13,16,17,20,66] One of these papers treats the resonant Auger decay of the photoexcited C $1s \rightarrow 2\pi$ CO molecule.[17] In this work, bound parts of the core-hole state and the final state were represented by the multireference configuration-interaction (CI) method using standard quantum chemical programs based on Gaussian basis functions.[54,55] The Auger continuum channel was obtained by solving the Lippmann–Schwinger equation in a basis set of atom-centered Gaussian functions. It was then expanded in a one-center expansion up to $l=6$ in order to extrapolate to the asymptotic behavior of the continuum channels. Further details on this approach are given in Refs. 13, 16, and 17. The C $1s^{-1}2\pi$ resonance of the CO molecule represents the only case for which reliable results are available for angular distributions of Auger electrons from both theoretical and experimental works.

The main purpose of this paper is to show that the comparatively simple one-center approximation provides good-quality angular distributions of Auger electrons in the molecular Auger decay. This approximation assumes that all molecular valence orbitals can be described as a linear combination of the atomic valence orbitals. The transition matrix elements are then transformed from the basis of the molecular orbitals to a basis of the atomic valence orbitals. All matrix elements that contain atomic orbitals not belonging to the atom at which the Auger decay happens are neglected and the remaining interatomic Auger transition matrix elements are taken from atomic calculations. The one-center approximation[27,28] was shown to describe spherically aver-

aged intensities of molecular Auger decay processes quite well (see Ref. 38 and references therein). More detailed recent comparisons[34] even indicate that these quantities are of the same accuracy as the generally much more demanding alternatives. A new aspect in applying the one-center approximation to the angular distribution of Auger electrons is that relative phases of the decay amplitudes are required. Potential difficulties for the one-center approximation lie in the fact that it neglects scattering effects of the Auger electron from the non-core-hole atoms in the molecule and, furthermore, cuts the angular expansion of the continuum channels. A justification for the latter fact is that the more advanced calculations in Refs. 12–17 indicate that the largest part of the angular distribution is properly represented by such a short expansion of the continuum channels: In Refs. 13, 16, and 17 the absolute values of the anisotropy parameters for all investigated final molecular states in the Auger decay of the *K*-hole in HF, HF$^+$, and CO molecules, sharply drop down after the first five values, which are only allowed in the simplest version of the one-center model. As shown below, these most significant values are properly obtained with the one-center approximation.

This manuscript is organized as follows. Section II presents a formalism of the angular distributions of Auger electrons in the resonant molecular Auger decay, including a convenient parameterization for the molecular frame Auger electron angular distribution (MFAAD) and outlines the main steps in their calculation within the one-center approximation. The method is applied in Sec. III to the resonant Auger decay of the photoexcited C $1s \rightarrow 2\pi$ CO molecule. These results are compared to experimental data and other theoretical calculations. Summary and concluding remarks are given in Sec. IV. Within this article atomic units are used throughout unless indicated otherwise.

II. THEORY

A. Basic equations

In this paper we consider the resonant Auger decay of a linear molecule initially in the $^1\Sigma$ state as a two-step process: photoexcitation in the inner shell by linearly polarized radiation to the $^1\Pi$ state (step 1) and subsequent Auger decay (step 2). The MFAAD is given by an expansion,[12–14] adapted to our case in the form

$$I_{\text{mol}}(\theta,\phi) = \sum_K \sum_{\Lambda,\Lambda'=\pm 1} \langle \Lambda'|\rho|\Lambda \rangle$$
$$\times A_K(\Lambda'\Lambda) \sqrt{\frac{4\pi}{2K+1}} Y^*_{K\Lambda'-\Lambda}(\theta,\phi), \quad (1)$$

where $Y_{lm}(\theta,\phi)$ is a spherical harmonic in the Condon–Shortley phase convention, $\langle \Lambda'|\rho|\Lambda \rangle$ is the density matrix of the Auger decaying state in the molecular frame, and $\Lambda(\Lambda')$ is the projection of the orbital angular momentum of the $^1\Pi$ state on the molecular axis, which is chosen as the z axis of the molecular frame. The xz plane is spanned by the molecular axis and the electric field. The dynamics of the Auger decay is contained in the anisotropy parameters $A_K(\Lambda'\Lambda)$ specific for each final molecular state f,

$$A_K(\Lambda'\Lambda) = \frac{1}{2\pi} \sum_{\substack{ll'mm' \\ \Lambda_f}} (-1)^{m'} \sqrt{(2l+1)(2l'+1)} (l0,l'0|K0)$$

$$\times (lm,l'-m'|K\Lambda-\Lambda') V_{\Lambda'\to\Lambda_f,l'm'} V^*_{\Lambda\to\Lambda_f,lm}, \quad (2)$$

where l and m are the orbital angular momentum of the Auger electron and its projection on the molecular axis, respectively; Λ_f is the projection of the orbital angular momentum of the molecular ion in the final state. The standard notation is used for the Clebsch–Gordan coefficients. $V_{\Lambda\to\Lambda_f,lm}$ denotes the Auger decay amplitude (independent on spin projections) in the molecular frame

$$V_{\Lambda\to\Lambda_f,lm} = \langle\Lambda_f,lm^{(-)}|\hat{H}-E|\Lambda\rangle_{S,S_f}, \quad (3)$$

where $\hat{H}$ is the molecular Hamiltonian and E is the total energy of the Auger decaying (core-hole) state. The subscripts S and S_f symbolize that the amplitude in Eq. (3) depends on the total spins of the initial molecular and the final molecular ion states and $(-)$ indicates that the asymptotic form of the continuum wave function is outgoing. Note that the rank K in Eq. (1) is limited by the number $2l_{max}$, where l_{max} is the largest orbital momentum component of the Auger electron. Generally, l_{max} is restricted only due to the decrease in the decay amplitude (3) with increasing l.

In the particular case of a quantum mechanically pure Auger decaying state, described by some state vector $|i\rangle$ (i.e., $\langle\Lambda'|\rho|\Lambda\rangle = \langle\Lambda'|i\rangle\langle i|\Lambda\rangle$) expression (1) can be written in an alternative contracted form. In our case, only core-excited states with zero projection of the angular momentum on the direction of the electric field **E** are excited, $|i\rangle = |\Lambda_E=0\rangle$. The reflection symmetry with respect to the xz plane gives $\langle\Lambda_E=0|\Lambda=1\rangle = \langle\Lambda_E=0|\Lambda=-1\rangle$ and after some algebra Eq. (1) simplifies to

$$I_{mol}(\theta,\phi,\theta_n) = N(\theta_n) \sum_{\Lambda_f} \left| \sum_{lm\Lambda} V_{\Lambda\to\Lambda_f,lm} Y_{lm}(\theta,\phi) \right|^2, \quad (4)$$

where the factor $N(\theta_n) = 2|\langle\Lambda_E=0|\Lambda=1\rangle|^2$ does not depend on the direction of the Auger emission in the molecular frame, but only on the angle θ_n between the molecular axis and the polarization of the incoming photon beam. The angular distribution of Auger electrons from a photoexcited free rotating molecule is of the form[8]

$$I(\vartheta) = \frac{I_0}{4\pi}[1 + \beta P_2(\cos\vartheta)], \quad (5)$$

where I_0 is the integral intensity of the Auger line (Auger transition rate), ϑ is the angle between the Auger electron emission and the electric field of the incident light, $P_2(\cos\vartheta)$ is the second Legendre polynomial, and β is the asymmetry parameter of the angular distribution of Auger electrons. The parameters of the angular distribution (5) are expressed in terms of the anisotropy parameters as

$$I_0 = 4\pi A_0(11), \quad (6)$$

$$\beta = -\frac{1}{5}\frac{A_2(11) + \sqrt{6}A_2(-11)}{A_0(11)}. \quad (7)$$

B. Parametrization of the MFAAD

A discussion of MFAADs (1) and (4) is simplified by establishing a set of their independent parameters. The resonant Auger decay is a particular case of photoionization. Therefore, it is instructive to take a general parametrization for the molecular frame photoelectron angular distribution (MFPAD),[67]

$$I_{ph}(\theta,\phi;\theta_n) = F_{00}(\theta) + F_{20}(\theta)P_2^0(\cos\theta_n)$$

$$+ F_{21}(\theta)P_2^1(\cos\theta_n)\cos\phi$$

$$+ F_{22}(\theta)P_2^2(\cos\theta_n)\cos 2\phi, \quad (8)$$

and find restrictions on the parameters due to the resonant character of the process. In Eq. (8), $P_L^N(\cos\theta_n)$ is the associated Legendre polynomial and $F_{LN}(\theta)$ are in general independent functions of θ.

By using standard density matrix and statistical tensor formalism,[25,68,69] Eq. (1) can be reduced to form (8) with

$$F_{00}(\theta) = \frac{2}{3}\sum_{K=0}^{\infty} A_K(11)P_K^0(\cos\theta), \quad (9)$$

$$F_{20}(\theta) = -\frac{2}{3}\sum_{K=0}^{\infty} A_K(11)P_K^0(\cos\theta) = -F_{00}(\theta), \quad (10)$$

$$F_{21}(\theta) = 0, \quad (11)$$

$$F_{22}(\theta) = -\frac{1}{3}\sum_{k=2}^{\infty} A_K(-11)\sqrt{\frac{(K-2)!}{(K+2)!}}P_K^2(\cos\theta). \quad (12)$$

Equation (8) is then simplified considerably for the MFAAD, giving

$$I_{mol}(\theta,\phi;\theta_n) = \frac{3}{2}\sin^2\theta_n(F_{00}(\theta) + 2F_{22}(\theta)\cos 2\phi). \quad (13)$$

It is explicitly seen that the azimuthal ϕ-dependence of the MFAAD is only due to coherent mixing of terms with different projections of the decaying state $\Lambda \neq \Lambda'$ on the molecular axis,[17] which are contained in $F_{22}(\theta)$. A further relation can be deduced for the special case of $\Lambda_f=0$. Substituting Eq. (2) into Eqs. (9) and (12), applying the Clebsch–Gordan expansion for spherical harmonics, evaluating the sum over K, and using the symmetry of the Auger decay amplitudes with respect to the xz plane, we finally obtain

$$F_{00}(\theta) = 2\eta_f F_{22}(\theta), \quad \text{for } \Lambda_f = 0, \quad (14)$$

where η_f is the spatial parity of the molecular ion $\Lambda_f=0$ state. As a result, for the MFAAD only one independent function of θ is left,

$$I_{mol}(\theta,\phi;\theta_n) = 3F_{00}(\theta)\sin^2\theta_n \begin{cases} \cos^2\phi & \text{for } \Lambda_f = \Sigma^+ \\ \sin^2\phi & \text{for } \Lambda_f = \Sigma^-. \end{cases}$$

$$(15)$$

A few conclusions follow from Eq. (13). Only a maximum of two independent functions, $F_{00}(\theta)$ and $F_{22}(\theta)$, describe the θ-dependence of the MFAAD in contrast to MFPAD (8) with generally four independent functions. The

dependence of the MFAAD on the direction of the polarization, i.e., on the angle θ_n between the polarization and the molecular axis, is factored out, in contrast to the general case of photoionization, described by Eq. (8). The shape of the MFAAD does not depend on the angle θ_n, which gives only a general modulation, with the strongest signal for the polarization perpendicular to the molecular axis and a vanishing signal when they are parallel. This natural result follows from the fact that the Auger magnetic substates with the projections $\Lambda = \pm 1$ are not excited in the latter case due to the selection rule. The θ_n-independent part of the MFAAD in Eq. (13) is equivalent to Eq. (8) of Bonhoff *et al.*[17] MFAAD (13) is symmetric with respect to the transformation $\theta_n \rightarrow \pi - \theta_n$. This is the result of the sharp absolute value of the projection $|\Lambda| = 1$. Any deviation from the $\theta_n \rightarrow \pi - \theta_n$ symmetry would indicate a contribution of the photoionization channel with $\Lambda = 0$ [through the term with the Legendre polynomial $P_2^1(\cos \theta_n)$ in Eq. (8)]. This gives a method of revealing a background of the direct photoionization, or of an overlapping Auger resonance with $\Lambda = 0$.

C. Method of calculation

In order to represent the Auger decay amplitude (3) in the one-center approximation we write them in the form

$$V_{\Lambda \rightarrow \Lambda_f, lm} = \exp i\delta_l A_{lm\Lambda}, \tag{16}$$

where δ_l is the phase shift of the Auger electron in the channel with orbital angular momentum l. In consistence with the atomic model underlying the one-center approximation, this phase shift is chosen to be independent of the magnetic quantum number m. In Eq. (16) we have introduced the amplitudes

$$A_{lm\Lambda} = \langle \mathcal{A}_S \Psi_{\Lambda_f S_f} \varphi_{\epsilon lm} | \hat{H} - E | \Psi_\Lambda \rangle, \tag{17}$$

where Ψ_Λ and $\Psi_{\Lambda_f S_f}$ are the intermediate (core-hole) and final state many-electron wave functions, respectively, and $\mathcal{A}_S$ designates an antisymmetrization and spin-adaptation operator.[29,36] $\varphi_{\epsilon lm}$ is the regular continuum wave function of the Auger electron with the energy ϵ,

$$\varphi_{\epsilon lm}(\mathbf{r}) = r^{-1} R_{\epsilon l}(r) Y_{lm}(\theta_r, \phi_r). \tag{18}$$

For the present purpose of resonant Auger decay, $\varphi_{\epsilon lm}$ is an atomic continuum wave function emitted from a C$^+$ cation with the kinetic energy of about 270 eV. In Eq. (18), the vector $\mathbf{r}$ corresponding to the spherical coordinates r, θ_r, and ϕ_r defines the position of the Auger electron with respect to the center of the core-hole atom, and $R_{\epsilon l}(r)$ is the real radial continuum wave function with the asymptotic form

$$\lim_{r \rightarrow \infty} R_{\epsilon l}(r) = \sqrt{\frac{2}{\pi k}} \sin\left(kr + \frac{1}{k}\ln(2kr) + \delta_l\right), \tag{19}$$

where $k = \sqrt{2\epsilon}$. Note that the thus defined phase shift δ_l automatically includes the Coulomb phase shift and the phase due to the short-range part of the potential. As described below, the phase shift δ_l is found by fitting the radial part of the calculated atomic continuum wave function $R_{\epsilon l}(r)$ to the asymptotic form of Eq. (19).

With the amplitudes from Eqs. (16) and (17) and the phase shifts δ_l of the Auger channels, the anisotropy parameters $A_K(\Lambda'\Lambda)$ can be calculated according to Eq. (2). The MFAAD and the asymmetry parameter can be found then from Eqs. (9), (12), (13), and (7), respectively. Alternatively, if only the shape of the MFAAD is to be found for a fixed-in-space molecular axis, Eqs. (4) and (16) can be used.

III. C 1s→2π PHOTOEXCITED CO AUGER DECAY

Here we apply the above described method to the angular distributions of Auger electrons in the resonant Auger decay of the C $1s \rightarrow 2\pi$ excited CO molecule. The corresponding angle integrated Auger decay spectrum of this molecule has been successfully treated by the one-center approximation.[5,35,70]

A. Calculational details

The Auger decay amplitudes in Eq. (17) are obtained from the wave functions of the intermediate and final electronic states as described previously.[29,31,36] In order to assess the sensitivity of the angular distributions on details of these wave functions, two different orbital sets were employed: The Hartree–Fock orbitals of the neutral ground state and those of the C $1s$-core-ionized state. Unless stated otherwise, all calculations were done at the equilibrium bond distance of the CO ground state $r_e = 1.1283$ Å.[71] The orbitals were represented with the cc-pVTZ basis set[72] and virtual valence orbitals were obtained as described in Ref. 38. The ground, core-excited, and final states were represented by CI wave functions including all possible configurations with the occupation pattern $(1\sigma^2 2\sigma^2 val^{10})$, $(1\sigma^2 2\sigma^1 val^{11})$, and $(1\sigma^2 2\sigma^2 val^9)$, respectively, where "val" stands for the valence orbitals $(3\sigma 4\sigma 1\pi 5\sigma 2\pi 6\sigma)$. A projection of the molecular orbitals on the atomic $1s$, $2s$, and $2p$ orbitals is performed as described earlier.[36,38] In any case these projected orbitals represent more than 98% of the density of the molecular orbitals. As the one-center approximation employs only the carbon $2s$ and $2p$ contributions of these orbitals, the Auger channels with angular momenta l up to 2 (s, p, and d) are possible in the present case.

The phase shifts δ_l needed for the calculation of the angular distributions of Auger electrons were obtained with the ATSP package.[73] s, p, and d continuum electron wave functions were calculated for different terms of the carbon ion C$^+$ configurations $[(1s^2 2s^2 2p^2)$, $(1s^2 2s^1 2p^3)$, and $(1s^2 2s^0 2p^4)]$ and different total orbital angular momenta and spin quantum numbers of the final state (C$^+$+electron). For the rather high Auger electron energies of interest (260–275 eV), the phase shift differences were found stable and not sensitive to the ionic state, the global quantum numbers, details of the bound orbitals, and the fitting range of the phase shifts. The latter was chosen to be about $4-8a_0$. Within 4° the above differences have the values $\delta_p - \delta_s = 208°$, $\delta_d - \delta_s = 95°$, and $\delta_d - \delta_p = -113°$, which were used in the present calculations. The major contribution to these differences comes from the short-range potential: the differences between the Coulomb phase shifts are $-13°$, $-19°$, and $-6°$, respectively.

TABLE I. Auger transition rates of the C $1s \rightarrow 2\pi$ excited state of CO to the indicated states of CO$^+$ as calculated with the present approach in comparison with other theoretical works. Leading configurations are given with respect to the ground state configuration of the CO molecule. All values in 10^{-3} a.u.

Term	Leading configuration	I_0 [a]	I_0 [b]	I_0 [c]	I_0 [d]	I_0 [e]
$(1)^2\Sigma^+$	$(5\sigma^{-1})$	0.154	0.133	0.188	0.114	0.107
$(2)^2\Pi$	$(1\pi^{-1})$	0.575	0.646	0.399	0.360	0.360
$(3)^2\Sigma^+$	$(4\sigma^{-1})$	0.031	0.032	0.090	0.073	0.073
$(4)^2\Pi$	$(5\sigma^{-2}2\pi^1)$	0.290	0.210	0.263	0.169	0.176
$(5)^2\Delta$	$(1\pi^{-1}5\sigma^{-1}2\pi^1)$	0.160	0.171	0.141	0.129	0.103
$(6)^2\Sigma^-$	$(1\pi^{-1}5\sigma^{-1}2\pi^1)$	0.051	0.049	0.059	0.048	0.037
$(7)^2\Sigma^+$	$(1\pi^{-1}5\sigma^{-1}2\pi^1)$	0.191	0.218	0.175	0.154	0.129
$(8)^2\Delta$	$(1\pi^{-1}5\sigma^{-1}2\pi^1)$	0.134	0.141		0.165	0.140
$(9)^2\Sigma^-$	$(1\pi^{-1}5\sigma^{-1}2\pi^1)$	0.093	0.100		0.092	0.081
$(10)^2\Pi$	$(1\pi^{-2}2\pi^1)$ [f]	0.314	0.235		0.584	0.459
$(11)^2\Pi$	$(1\pi^{-2}2\pi^1)$ [f]	0.316	0.269		0.154	0.136
$(12)^2\Pi$	$(4\sigma^{-1}5\sigma^{-1}2\pi^1)$ [f]	0.040	0.197			
$(13)^2\Phi$	$(1\pi^{-2}2\pi^1)$	0.029	0.040			

[a]This work, CO ground state orbitals.
[b]This work, orbitals of the C $1s$ ionized state of CO.
[c]Theoretical values from Bonhoff *et al.* (Ref. 17).
[d]Theoretical "two channel" values from Botting and Lucchese (Ref. 53).
[e]Theoretical "five channel" values from Botting and Lucchese (Ref. 53).
[f]These $^2\Pi$ states show significant configuration mixing (see the text).

B. Final states and spherically averaged intensities

Table I presents the line intensities of the 13 relevant final states for the main structures in the resonant Auger spectrum as obtained with the present calculations and the theoretical results of Bonhoff *et al.*[17] and of Botting and Lucchese.[53] The first two columns show the terms and leading configurations of the final CO$^+$ states. There and in the following, configurations are given with respect to the leading configuration of the neutral ground state $(1\sigma^2 2\sigma^2 3\sigma^2 4\sigma^2 1\pi^4 5\sigma^2)$. The states are numbered according to their energies. This numbering is unambiguous for the first three states but due to curve crossings at about the equilibrium bond distance, already the ordering of the states $(4)^2\Pi$, $(5)^2\Delta$, and $(6)^2\Sigma^-$ depends strongly on details of the calculation such as the bond distance or the chosen configuration and orbital spaces. As discussed before in Ref. 70 the $(10-12)^2\Pi$ states show a series of avoided crossings at about the equilibrium bond distance. As they have the same terms, the leading configuration of the states is a strong function of the parameters of the calculation. A more detailed analysis of the final states[74] shows that the by far largest part of their intensity is due to a diabatic state with the leading configuration $(4\sigma^{-1}5\sigma^{-1}[^1\Sigma^+]2\pi^1)$. This configuration interacts with configurations of the type $(1\pi^{-2}2\pi^1)$ [i.e., $(1\pi^{-2}[^3\Sigma^-]2\pi^1)$, $(1\pi^{-2}[^1\Delta]2\pi^1)$, and $(1\pi^{-2}[^1\Sigma^+]2\pi^1)$] and the configuration $(4\sigma^{-1}5\sigma^{-1}[^3\Sigma^+]2\pi^1)$. In these configuration notations the terms in brackets indicate the coupling of the two holes which couple with the 2π electron to the $^2\Pi$ term. Note that the $(10-12)^2\Pi$ states are all strong mixtures of these configurations and that the $(4\sigma^{-1}5\sigma^{-1}[^1\Sigma^+]2\pi^1)$ configuration contributing most to the Auger intensity is mostly hidden in this configuration mixing.

Table I shows that the different theoretical approaches provide essentially similar results for the transition rates. The present one-center approximation results tend to provide larger transition rates than the other works. We assign this effect to the use of the initial state atomic transition integrals of Chen *et al.*,[75] which tended to overestimate true Auger transition rates.[37,44] However, variations in the approximations for the bound part of the wave functions such as the use of different orbital sets in the present work or the use of different numbers of channels in the work of Botting and Lucchese[53] cause changes in the transition rates for about 20%. This is the same order of magnitude as the differences between the one-center and the multichannel approaches. Thus, from the present results, but also from preceding investigations,[27,31,35,76,77] it can be stated that the treatment of the continuum channels via the one-center approximation does not cause larger uncertainties in calculated Auger transition rates than other inherent approximations within all presently available approaches. In Secs. III C and III D we will investigate whether this holds also for the predictions of the angular distribution of the Auger electrons.

C. Angular distributions from fixed-in-space molecules

It is implied in the following that the origin of the molecular frame coincides with the carbon atom and the z-axis points in the direction of the oxygen atom. Discussing the MFAADs, one has to keep in mind that in practice only dissociative states with sufficiently high energies of the fragments can be experimentally studied by the Auger electron—ion recoil coincidence technique. Among the states listed in Table I only those which give rise to spectator-type Auger decay $(5)^2\Delta$, $(6)^2\Sigma^-$, $(8)^2\Delta$, $(9)^2\Sigma^-$, $(13)^2\Phi$, and $(10-12)^2\Pi$ are dissociative.[78] In other cases, to observe the MFAADs, the molecule should be fixed in space by other means, e.g., by adsorption on a surface.[1]

The MFAADs are completely determined by the sets of anisotropy parameters $A_K(11)$ and $A_K(-11)$ or by the functions $F_{00}(\theta)$ and $F_{22}(\theta)$. In Table II we have listed the non-

TABLE II. Anisotropy parameters for the Auger decay of the C $1s^{-1}2\pi$ resonance in 10^{-5} a.u.

K	$(1)^2\Sigma^+$	$(2)^2\Pi$	$(3)^2\Sigma^+$	$(4)^2\Pi$	$(5)^2\Delta$	$(6)^2\Sigma^-$	$(7)^2\Sigma^+$	$(8)^2\Delta$	$(9)^2\Sigma^-$	$(10)^2\Pi$	$(11)^2\Pi$	$(12)^2\Pi$	$(13)^2\Phi$
						$A_K(11)$							
0	1.2257	4.5740	0.2473	2.3053	1.2755	0.4035	1.5208	1.0661	0.7390	2.4976	2.5179	0.3176	0.2283
1	0.1893	−0.6159	−0.0971	−3.1081	−0.6663	−0.2095	−0.7355	−0.3312	−0.2809	−3.4106	−3.1135	0.4071	0.0000
2	0.8289	−3.7386	0.1050	3.5077	−0.2730	−0.0095	−0.7203	−0.8882	−0.5418	1.1083	0.7956	0.3894	−0.3260
3	−0.1893	−0.2338	0.0971	−1.4937	0.6663	0.2095	0.7355	0.3312	0.2809	−0.3875	−0.0970	−0.0805	0.0000
4	−2.0546	2.9172	−0.3523	1.1497	−1.0025	−0.3940	−0.8006	−0.1779	−0.1972	0.2078	0.1482	0.0283	0.0979
						$A_K(-11)$							
2	−2.1636	−4.5813	−0.4619	0.3230	⋯	0.8275	−3.3985	⋯	1.7296	−0.1737	0.3824	0.0038	⋯
3	−0.3456	−0.3878	0.1774	0.2548	⋯	−0.3824	1.3428	⋯	−0.5128	−0.1358	0.6111	0.0137	⋯
4	−3.2487	4.5913	−0.5571	−0.3367	⋯	0.6229	−1.2658	⋯	0.3118	0.1217	−0.1253	−0.0083	⋯

vanishing anisotropy parameters calculated in the one-center model for the 13 transitions considered in the present work. As noted by Bonhoff *et al.*,[16,17] the anisotropy parameters up to $K=4$ are dominant. In our model, which includes only s, p, and d continuum channels, the anisotropy parameters with $K>4$ are strictly zero.

Note that for the final states with projections $\Lambda_f \geq 2$ (Δ and Φ states), the nondiagonal anisotropy parameters $A_K(-11)$ vanish in our model. This is seen from Eq. (2), where one of the decay amplitudes will turn to zero because of the conservation of the angular momentum projection and the restriction $l, l' \leq 2$. Therefore, the function $F_{22}(\theta)$ in Eq. (13) vanishes and the MFAADs become cylindrically symmetric with respect to the molecular axis. Although this is a model dependent result, in view of a general decrease in the contributions with increasing l, it is reliable and consistent with the results of Bonhoff *et al.*[17] that MFAADs became essentially cylindrically symmetric for $\Lambda_f \geq 2$, i.e., Δ and Φ final states.

Figure 1 compares the three-dimensional (3D) spherical plots of the MFAADs obtained in our one-center model with the calculations of Bonhoff *et al.*,[17] where the anisotropy parameters were presented for the seven lowest final states. The agreement between the two theoretical results in general is very good. The existing discrepancies are not due to the smaller number of the anisotropy parameters A_K ($K \leq 4$) in our model: this was checked by truncating the number of these parameters given by Bonhoff *et al.*[17] from $K_{max}=8$ to $K_{max}=4$. Rather, the deviations are due to the different models for the calculations of the decay amplitudes. While the approach of Bonhoff *et al.*[17] described the physical details of the Auger process more accurately, it is very much more laborious.[13] Additionally, it contains numerically delicate and computationally demanding steps as the representation of a multicenter continuum wave function with a square integrable Gaussian basis, transformations from the multicenter basis set to a one-center expansion, and the diagonalization of a large CI-expansion for several final states. It is noticeable from Fig. 1 that the major differences in the MFAADs obtained in the two models are located in the direction of the oxygen atom. Possibly, it reflects the lack of rescattering of the Auger electron wave by the oxygen atom in our one-center model. Nevertheless, the angular distributions obtained in the present work and by Bonhoff *et al.*[17] are re-

markably similar and in face of the still very limited theoretical and experimental materials available so far, the differences between the results must be considered as marginal.

The MFAADs for the remaining six states of the manifold are shown in Figs. 2 and 3 as 3D spherical plots together with graphs of the MFAADs as functions of the polar angle θ for various fixed values of the azimuthal angle ϕ. Some characteristic features of the MFAADs for different final states are seen clearly in Figs. 1–3, revealing the stereodynamics of the Auger decay.[17] The MFAADs corresponding to the Auger decay to the $^2\Sigma$ states show a "butterflylike" pattern concentrated either in the same plane as the electric field for the $^2\Sigma^+$ states, or in the normal plane for the $^2\Sigma^-$ states, in accordance with Eq. (15). This form is due to the fact that the outgoing channels have exclusively p_x and d_{xz} (p_y and d_{yz}) characters for the $^2\Sigma^+$ ($^2\Sigma^-$) final states. The p contribution reflects the participation of $2s$-character on the valence orbital from which an electron is extracted in the Auger pro-
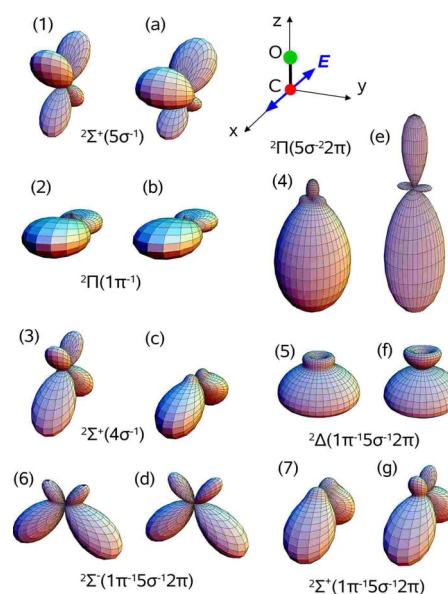

FIG. 1. (Color online) The MFAADs of the seven lowest final states. Numbers (1)–(7) designate the results of the present investigation and correspond to the numbers of the CO$^+$ states in Tables I and II. Labels (a)–(g) mark the corresponding results of Bonhoff *et al.* (Ref. 17). The electric field vector points in the x direction of the molecular frame, which is shown in the inset.
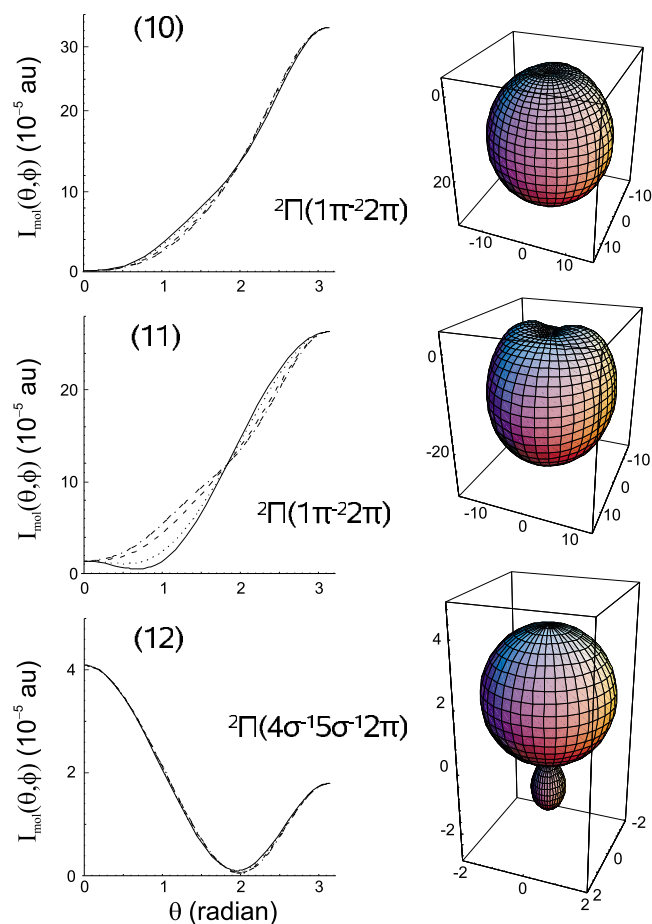
FIG. 2. (Color online) MFAADs [Eq. (13)] from the present one-center calculations for the (10–12)$^2\Pi$ final states of CO$^+$. The numbers correspond to those in Tables I and II. Right column: 3D spherical plots. Left column: the MFAADs as a function of θ for various fixed values of ϕ. Solid line: $\phi=0°$, dotted line: $\phi=30°$, dashed line: $\phi=60°$, dashed-dotted line: $\phi=90°$. The orientation of the CO molecule and the direction of the electric field $\boldsymbol{E}$ are chosen as shown in Fig. 1.

cess while the d contribution reflects the corresponding $2p$ character of this valence orbital. The d character (butterfly-like shape) of the continuum channels shows that the $2p$-character participates more effectively.

The shapes of the MFAADs for the final $^2\Pi$ states differ crucially for the participator decay [state (2), see Fig. 1] and the spectator decay [state (4), see Fig. 1 and states (10–12), see Fig. 2]. A detailed explanation of the MFAADs of the $^2\Pi$ final states is more involved than for the $^2\Sigma$ states. Altogether, five channels s, p_z, $d_{x^2-y^2}$, d_{z^2}, and d_{xy} are populated in the decay to these final states. For the participator transition, the latter channel is populated via the decay of the core-excited state with preferential occupation of the $2\pi_x$ orbital to a $^2\Pi$ final state of CO$^+$ with the $1\pi_y$ hole. Due to symmetry reasons, the channels corresponding to this component of the "$^2\Pi_y$" final state do not interfere with those of the degenerate "$^2\Pi_x$" component. The form of the MFAAD for the latter component depends strongly on the channel interference of the remaining channels, which contain s, p, and d characters. Thus, the result for the MFAAD for the $^2\Pi$ final state from a theoretical method is heavily dependent on its ability to represent the channel amplitudes *and* their phase shifts.
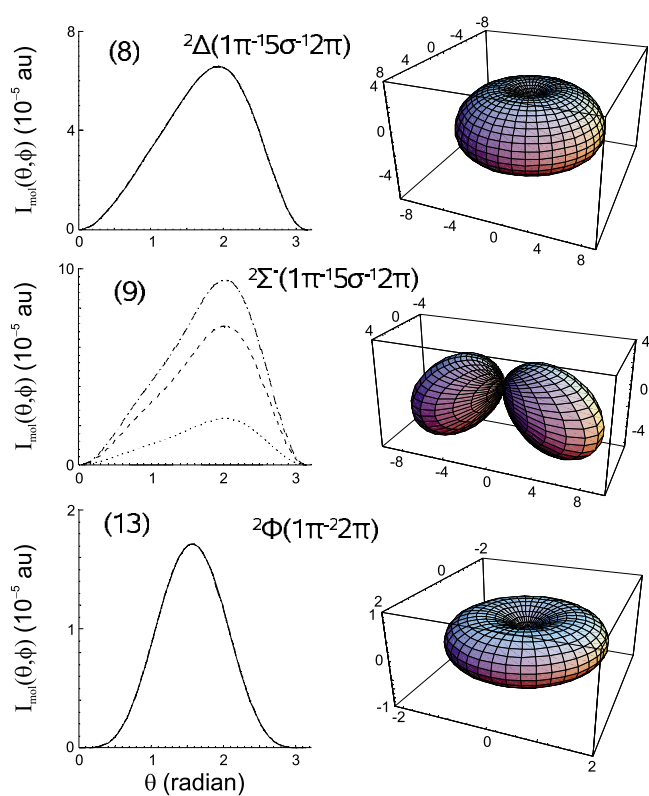

FIG. 3. (Color online) As in Fig. 2 but for (8)$^2\Delta$, (9)$^2\Sigma^-$, and (13)$^2\Phi$ final states.

For the spectator transitions to the $^2\Pi$ states (4) and (10–12), the MFAAD is dominated by transitions in which one electron is staying in the 2π orbital while the actual Auger decay takes place for valence electrons such that a $^1\Sigma^+$ or $^1\Delta$ valence configuration is obtained for the orbitals occupied in the ground state configuration. In this case, the d_{xy} and $d_{x^2-y^2}$ channels are only weak and the largest part of the Auger decay is due to the s, p_z, and d_{z^2} channels with σ-symmetry. Accordingly, all of these MFAADs are essentially symmetric with respect to rotation about the molecular axis. It is particularly remarkable, that there is a very strong preference for emission of the Auger electron in the direction opposite to the oxygen atom. Such a preference indicates significant interference effects between the nonorthogonal decay amplitudes for the s and p_z channels (as mentioned above, $\delta_p - \delta_s = 208°$).

The MFAADs for the $^2\Delta$ and $^2\Phi$ final CO$^+$ states (8) and (13) presented in Fig. 3 are cylindrically symmetric, as discussed above, and concentrated in the equatorial plane of the molecular frame.

D. Angular distributions from rotating molecules

The results for the asymmetry parameter β for the Auger decay of the C $1s^{-1}2\pi$ resonance to the considered final states of the molecular ion CO$^+$ are collected in Table III. We compare our results with theoretical values of Bonhoff *et al.*[17] and the asymmetry parameters measured by Hemmers *et al.*[3] and by Kukk *et al.*[5] In view of the discussion of the MFAADs, it is not surprising that our calculations give re-

TABLE III. Asymmetry parameters from the present approach and from prior work.

N	Term	β [a]	β [b]	β [c]	β_{exp} [d]	β_{exp} [e]
(1)	$^2\Sigma^+$	0.730	0.731	0.820	0.79	0.78(2)
(2)	$^2\Pi$	0.654	0.649	0.997	0.67	0.70(2)
(3)	$^2\Sigma^+$	0.830	0.851	1.170	1.10	0.97(2)
(4)	$^2\Pi$	−0.373	−0.412	−0.535		<−0.5
(5)	$^2\Delta$	0.043	0.058	−0.051		
(6)	$^2\Sigma^-$	−1.000	−1.000	−1.000		
(5)+(6) [f]		−0.209	−0.197	−0.366		>−0.3
(7)	$^2\Sigma^+$	1.189	1.179	1.000		>0.6
(8)	$^2\Delta$	0.167	0.160			
(9)	$^2\Sigma^-$	−1.000	−1.000			
(8)+(9) [f]		−0.311	−0.321			<−0.15
(4)–(9) [f]	First spectator	0.005	0.061	−0.050		−0.22(2)
(10)	$^2\Pi$	−0.055	−0.093			
(11)	$^2\Pi$	−0.138	−0.245			
(12)	$^2\Pi$	−0.251	0.011			
(13)	$^2\Phi$	0.285	0.294			
(10)–(13) [f]	Second spectator	−0.090	−0.100			−0.14(3)

[a]This work, CO ground state orbitals.
[b]This work, orbitals of the C $1s$-ionized CO molecule.
[c]Theoretical value from Bonhoff *et al.* (Ref. 17).
[d]Experimental value from Hemmers *et al.* (Ref. 3).
[e]Experimental value after excitation in the $\nu=0$ band of the CO $1 s^{-1}2\pi$ state from Kukk *et al.* (Ref. 5).
[f]Intenstiy averaged β-values. $\beta_{av}=\Sigma_i\beta(i)I_0(i)/\Sigma_iI_0(i)$.

sults generally close to those of Bonhoff *et al.*[17] Both approaches are in good accordance with the experimental data available.

Positive values of β correspond to the preferential emission in the direction of the electric field, while negative values of β indicate preferential Auger emission in the plane, normal to the electric field. The β values are near to zero for the $^2\Delta$ and $^2\Phi$ final states, when the Auger electron is ejected in a symmetric fashion. It was already recognized and explained by Bonhoff *et al.*[17] from symmetry reasons that the β parameter is always −1 for decay into $^2\Sigma^-$ final states [states (6) and (9)]. It follows also directly from Eq. (15) (lower part), which shows that the Auger electrons are not emitted in the direction of the electric field vector, i.e., electron flux Eq. (5) vanishes at $\vartheta=0°$.

For a comparison of the calculated β values with the experimental data, the bond length dependence of these values was investigated with the present approach and CO ground state orbitals. The calculated asymmetry parameters turned out to be extremely weak functions of the CO bond distance: β values calculated at about the inner and outer probability maxima of the $\nu=2$ state of the core-excited state at $r=1.08$ Å and $r=1.25$ Å do not change by more than 0.01 units. The only exceptions are for the transitions to the $(10–12)^2\Pi$ and the $(3)^2\Sigma^+$ states. The former states change their character substantially due to the avoided crossings of the diabatic states in this region.[70] Thus, such changes are expected. However, the β value averaged over the $(10–12)^2\Pi$ states is again essentially bond distance independent.

The most prominent transitions in the resonant Auger electron spectrum of the C $1s^{-1}2\pi$ excited CO molecule are the participator transitions to the states numbered (1)–(3). The present theoretical approach and that one of Bonhoff *et*

al.[17] predicted very similar β values for the $(1)^2\Sigma^+$ final state which are about 0.05 units smaller and larger, respectively, than the experimental values. For the more intense $(2)^2\Pi$ state the asymmetry parameter β of Bonhoff *et al.*[17] is by about 0.3 larger than the experimental values, while the present approach is only about 0.05 units below these data.

For the particular transition to the $(3)^2\Sigma^+$ state it has been mentioned before by Kukk *et al.*[5] that the measured β-parameter is influenced by direct photoionization which has a large β-parameter of 1.8(2).[5] This admixture increases the asymmetry parameter and explains the relatively large difference between the value of $\beta=0.97(2)$ published by Kukk *et al.*[5] and the value of $\beta=1.10$ of Hemmers *et al.*[3] As the high resolution data of Kukk *et al.*[5] contained less contributions of direct photoionization than the data of Hemmers *et al.*,[3] they are probably the best numbers to compare with the theoretical data from this work and also from Bonhoff *et al.*[17]

For this $(3)^2\Sigma^+$ state, our theory shows an unusual increase of the transition rate as well as the β value with the bond distance. For $r_e=1.1283$ Å $(r=1.25$ Å), these values amount to $I_0=31$ μa.u. $(I_0=63$ μa.u.) and $\beta=0.830$ $(\beta=0.926)$. The intensity and asymmetry parameter change can be attributed to the special character of this participator transition. For the comparable N $1s^{-1}1\pi_g \rightarrow B^2\Sigma_u^+(2\sigma_u^{-1})$ transition of the N_2 molecule it was shown[79] that it changes from a participator transition at about equilibrium bond distance to a spectator transition at larger bond distances. The same also holds true for the CO molecule. With increasing bond length, the $(1\pi^{-1}5\sigma^{-1}2\pi^1)$ configuration that dominates the $(7)^2\Sigma^+$ state gains weight in the wave function of the $(3)^2\Sigma^+$. Simultaneously also the transition rate and asymmetry parameter increases. Thus, our calculated value of $\beta=0.830$ at the equi-

librium bond distance of the CO ground state should be corrected by an appropriate averaging over the vibrational motion. If this is taken into account the β value increases to 0.87.

On the basis of these considerations, the calculated value ($\beta=1.170$) of Bonhoff et al.,[17] for which the same corrections apply, must overestimate the actual value. Thus, the quite good agreement of the theoretical value $\beta=1.17$ of Bonhoff et al.,[17] with the experimental result, $\beta=1.10$, of Hemmers et al.[3] looks as an artifact. The probably more appropriate value is $\beta=0.97(2)$ of Kukk et al.[5] which is in reasonable agreement with the present vibrationally corrected result, $\beta=0.87$.

A comparison of the spectator region is more difficult as the individual final states cannot be detected experimentally due to overlap in the transitions. One particular case is that of the dissociative states $(5)^2\Delta$ and $(6)^2\Sigma^-$. They form almost energetically degenerate, parallel curves and, thus, provide a single and broad band in the resonant Auger spectrum that cannot be resolved experimentally. The same also happens for the $(8)^2\Delta$ and $(9)^2\Sigma^-$ states. Kukk et al.[5] provided upper and lower bounds for some groups of these states. According to this, the β value of the $(4)^2\Pi$ state should be smaller than -0.5. This is consistent with the results of Bonhoff et al.[17] (-0.535) but not with the present values that are around -0.4. The intensity averaged β value for the $(5)^2\Delta$ and $(6)^2\Sigma^-$ states is measured to be larger than -0.3 by Kukk et al.[5] which is consistent with the present theory ($\beta=-0.209$ and $\beta=-0.179$ for CO ground state and C $1s^{-1}$ orbitals, respectively) but not with the results of Bonhoff et al.[17] ($\beta=-0.366$). For the remaining states Kukk et al.[5] predicted the β value of the $(7)^2\Sigma^+$ state to be larger than 0.6 and the intensity averaged value of the $(8)^2\Delta$ and $(9)^2\Sigma^-$ states of less than -0.15. Both numbers are consistent with the present calculations ($\beta=1.18$ and $\beta=-0.32$, respectively) and with the asymmetry parameter of Bonhoff et al.[17] for the $(7)^2\Sigma^+$ state (1.00). However, for the intensity averaged asymmetry parameter of states $(4-9)$ which all contribute to the first spectator structure, Kukk et al.[5] reported a value of $\beta=-0.22(2)$. The corresponding theoretical value of the present work is 0.03 and that of Bonhoff et al.[17] is -0.05. The latter number should be lowered by about 0.05 as the calculations of Bonhoff et al.[17] did not include the $(8)^2\Delta$ and $(9)^2\Sigma^-$ states which have, in average, a negative contribution to the asymmetry parameter. While this indicates a slightly smaller error of the latter theory, we would like to mention that the experimental averaged asymmetry parameter of the second spectator structure shows a rather unexpected property: If the excitation energy was tuned to the maximum of the $v=1$ vibrational peak of the core-excited state, a value of $\beta=-0.12(2)$ was obtained for the averaged asymmetry parameter. Such a strong variation is not reported for any of the other β-values in the work of Kukk et al.[5] This is rather puzzling as direct photoionization plays only a minor role for these spectator states and as the present theoretical results indicate that the bond length dependence of the asymmetry parameters is essentially negligible. It may be anticipated that the theoretical approaches do not perform similarly well for spectator transitions. However, the intensity averaged

β-value of the second spectator group $[(10-12)^2\Pi$ and $(13)^2\Phi]$, $\beta\approx-0.10$, agrees rather well with the number of Kukk et al.,[5] $\beta=-0.14(3)$ for $v=0$. For this transition the experimental numbers are also much less dependent on the excitation energy. Kukk et al.[5] reported an averaged β value of $-0.12(3)$ for $v=1$.

IV. SUMMARY AND CONCLUSIONS

We have presented a simple approach to MFAADs based on the one-center approximation. The model incorporates atomic phase shifts into the one-center model of the Auger decay to describe the complex amplitudes. The method is very practical for calculations of the Auger electron angular distributions, since the absolute values of the Auger decay matrix elements are tabulated for many key cases.[32,75] Furthermore, the phase shifts can be obtained by standard atomic codes, especially as they do not require advanced atomic models for the high energy Auger electrons.

The theoretical framework of MFAADs is reformulated in a form that is appropriate for the one-center approximation. A parametrization of the MFAAD in the photoinduced resonant Auger is suggested, which is a particular case of the photoelectron molecular frame angular distribution, however with a reduced number of parameters. The angular distributions show features specific to final ionic molecular states.

The new one-center approach to MFAAD was applied to the benchmark example of resonant Auger decay: The photoexcited C $1s^{-1}2\pi$ resonance in carbon monoxide. The anisotropy parameters were calculated, which define the angular distributions of Auger electrons for both rotating and fixed-in-space molecules. The calculated Auger electron distributions from the fixed-in-space molecule are in good agreement with the preceding theoretical benchmark results of Bonhoff et al.[17] A qualitative interpretation of the MFAADs is given, indicating that for the case of the C $1s\to2\pi$ excited CO molecule, transitions to $^2\Pi$ final states are most sensitive to inherent parameters of a theoretical model.

The theoretical and experimental asymmetry parameters (β) of the angular distribution of Auger electrons from the partially oriented photoexcited C $1s\to2\pi$ CO molecules are critically compared to each other. For the isolated and therefore well defined participator transitions the present theoretical results deviate from the most reliable experimental data by less than 0.1. This is smaller than the deviation of the theoretically more advanced method of Bonhoff et al.[17] which is about 0.3. While the present results show a bit larger deviations (≈0.2) for the first group of spectator transitions, they perform very well for the second group of spectator transitions. Thus, as other theoretical asymmetry parameters are not available, the one-center approximation was unexpectedly found to provide MFAADs of so far unmatched accuracy for this benchmark case. If this is not an artifact, it means that a proper determination of the continuum wave functions in the nonspherical molecular field and backscattering of the Auger electron is less important for this property than so far undetermined error sources in the otherwise very advanced and reliable scattering approach in Refs. 12–17. It must be noted that the theoretical prediction

of a molecular Auger electron spectrum on the latter level of theory is by orders of magnitude more demanding than at the level of the one-center approximation. Thus, the one-center approach is applicable to extended systems such as liquids,[33,80] extended molecules,[41,81–83] and surfaces,[84,85] which are all far outside of the scope of comparable scattering approaches. With the additional capability of predicting angular distributions of Auger electrons, the one-center approximation could become the presently missing tool that allows one to interpret the information contained in the angular distribution of Auger electrons of, e.g., surface samples in material science.[2]

These results have several important consequences that demand further, partially already ongoing work. The present results should be verified with other theoretical and experimental methods. The MFAADs of fixed-in-space molecules and of adsorbates seem to offer reasonable possibilities for an experimental test. In particular, the second spectator group of transitions from the present study is a promising candidate for such experiments as the corresponding final states are rapidly dissociating. To reveal the range of its validity, the present approach should be also checked against asymmetry parameters of resonant Auger spectra using consistently detected experimental data. For this purpose, new experimental data may be necessary, as the present investigation indicated possible error sources in older, less resolved experiments. A generalization of the presented approach is currently developed which allows treating the resonant and normal Auger decay of other elements and of different angular momenta in the core holes.

ACKNOWLEDGMENTS

[1] P. Maciejewski, U. Höfer, W. Wurth, and E. Umbach, J. Electron Spectrosc. Relat. Phenom. **62**, 1 (1993).
[2] P. A. Brühwiler, O. Karis, and N. Mårtensson, Rev. Mod. Phys. **74**, 703 (2002).
[3] O. Hemmers, F. Heiser, J. Eiben, R. Wehlitz, and U. Becker, Phys. Rev. Lett. **71**, 987 (1993).
[4] O. Hemmers, S. B. Whitfield, N. Berrah, B. Langer, R. Wehlitz, and U. Becker, J. Phys. B **28**, L693 (1995).
[5] E. Kukk, J. D. Bozek, W.-T. Cheng, R. F. Fink, A. A. Wills, and N. Berrah, J. Chem. Phys. **111**, 9642 (1999).
[6] R. Guillemin, E. Shigemasa, K. Le Guen, D. Ceolin, C. Miron, N. Leclercq, P. Morin, and M. Simon, Phys. Rev. Lett. **87**, 203001 (2001).
[7] T. Weber, M. Weckenbrock, M. Balser, L. Schmidt, O. Jagutzki, W. Arnold, O. Hohn, M. Schöffler, E. Arenholz, T. Young, T. Osipov, L. Foucar, A. de Fanis, R. Díez Muiño, H. Schmidt-Böcking, C. L. Cocke, M. H. Prior, and R. Dörner, Phys. Rev. Lett. **90**, 153003 (2003).
[8] D. Dill, J. R. Swanson, S. Wallace, and J. L. Dehmer, Phys. Rev. Lett. **45**, 1393 (1980).
[9] S. Chapman, Adv. Chem. Phys. **82**, 432 (1992).
[10] K. Zähringer, H.-D. Meyer, and L. S. Cederbaum, Phys. Rev. A **46**, 5643 (1992).
[11] V. Kuznetsov and N. Cherepkov, J. Electron Spectrosc. Relat. Phenom. **79**, 437 (1996).
[12] K. Bonhoff, S. Nahrup, B. Lohmann, and K. Blum, J. Chem. Phys. **104**, 7921 (1996).
[13] B. S. S. Bonhoff, K. Bonhoff, and B. Nestmann, J. Phys. B **30**, 2821 (1997).
[14] J. Lehmann and K. Blum, J. Phys. B **30**, 633 (1997).
[15] A. Busalla and K. Blum, J. Phys. Chem. A **101**, 7476 (1997).
[16] K. Bonhoff, S. Bonhoff, B. Schimmelpfennig, B. Nestmann, and K. Blum, J. Phys. B **31**, 1511 (1998).
[17] S. Bonhoff, K. Bonhoff, and K. Blum, J. Phys. B **32**, 1139 (1999).
[18] N. M. Kabachnik, K. Ueda, Y. Muramatsu, and Y. Sato, J. Phys. B **31**, 4791 (1998).
[19] T. Kerkau and V. Schmidt, J. Phys. B **34**, 839 (2001).
[20] S. K. Semenov, V. V. Kuznetsov, N. A. Cherepkov, P. Bolognesi, V. Feyer, A. Lahmam-Bennani, M. E. S. Casagrande, and L. Avaldi, Phys. Rev. A **75**, 032707 (2007); see also publishers note in S. K. Semenov, V. V. Kuznetsov, N. A. Cherepkov, P. Bolognesi, V. Feyer, A. Lahmam-Bennani, M. E. S. Casagrande, and L. Avaldi, *ibid.* **75**, 059906 (2007).
[21] G. Wentzel, Z. Phys. **43**, 524 (1927).
[22] W. Mehlhorn, AIP Conf. Proc. **215**, 465 (1990).
[23] T. Åberg and G. Howart, in *Encyclopedia of Physics*, edited by W. Mehlhorn (Springer, Berlin, 1982), 31, Chap. 6, pp. 469–619.
[24] N. Kabachnik, S. Fritzsche, A. Grum-Grzhimailo, M. Meyer, and K. Ueda, Phys. Rep. **451**, 155 (2007).
[25] K. Blum, *Density Matrix Theory and Applications*, 2nd ed. (Plenum, New York, 1996).
[26] I. Hjelte, L. Karlsson, S. Svensson, A. D. Fanis, V. Carravetta, N. Saito, M. Kitajima, H. Tanaka, H. Yoshida, A. Hiraya, I. Koyano, K. Ueda, and M. N. Piancastelli, J. Chem. Phys. **122**, 084306 (2005).
[27] H. Siegbahn, L. Asplund, and P. Kelfve, Chem. Phys. Lett. **35**, 330 (1975).
[28] H. Ågren, S. Svensson, and U. Wahlgren, Chem. Phys. Lett. **35**, 336 (1975).
[29] H. Ågren, J. Chem. Phys. **75**, 1267 (1981).
[30] F. P. Larkins, Nucl. Instrum. Methods Phys. Res. B **87**, 215 (1994).
[31] H. Ågren, A. Cesar, and C.-M. Liegener, Adv. Quantum Chem. **23**, 1 (1992).
[32] E. Z. Chelkowska and F. P. Larkins, At. Data Nucl. Data Tables **49**, 121 (1991).
[33] G. Öhrwall, R. F. Fink, M. Tchaplyguine, L. Ojamae, M. Lundwall, R. R. T. Marinho, A. N. de Brito, S. L. Sorensen, M. Gisselbrecht, R. Feifel, T. Rander, A. Lindblad, J. Schulz, L. Sæthre, N. Mårtensson, S. Svensson, and O. Björneholm, J. Chem. Phys. **123**, 054310 (2005).
[34] Z. Bao, R. F. Fink, O. Travnikova, D. Céolin, S. Svensson, and M. N. Piancastelli, J. Phys. B **41**, 125101 (2008).
[35] H.-J. Freund and C.-M. Liegener, Chem. Phys. Lett. **134**, 70 (1987).
[36] R. Fink, J. Electron Spectrosc. Relat. Phenom. **76**, 295 (1995).
[37] R. F. Fink, M. Kivilompolo, H. Aksela, and S. Aksela, Phys. Rev. A **58**, 1988 (1998).
[38] R. F. Fink, S. L. Sorensen, A. Naves de Brito, A. Ausmees, and S. Svensson, J. Chem. Phys. **112**, 6666 (2000).
[39] O. M. Kvalheim, Chem. Phys. Lett. **98**, 457 (1983).
[40] F. P. Larkins, E. Z. Chelkowska, Y. Sato, K. Ueda, E. Shigemasa, and A. Yagishita, J. Phys. B **26**, 1479 (1993).
[41] M. Kivilompolo, A. Kivimäki, H. Aksela, M. Huttula, S. Aksela, and R. F. Fink, J. Chem. Phys. **113**, 662 (2000).
[42] S. Svensson, A. Ausmees, S. J. Osborne, G. Bray, F. Gel'mukhanov, H. Ågren, A. Naves de Brito, O.-P. Sairanen, E. Nõmmiste, H. Aksela, and S. Aksela, Phys. Rev. Lett. **72**, 3021 (1994).
[43] F. Gel'mukhanov, H. Ågren, S. Svensson, H. Aksela, and S. Aksela, Phys. Rev. A **53**, 1379 (1996).
[44] M. Kivilompolo, A. Kivimäki, M. Jurvansuu, H. Aksela, S. Aksela, and R. F. Fink, J. Phys. B **33**, L157 (2000).
[45] R. F. Fink, F. Burmeister, R. Feifel, M. Bässler, O. Björneholm, L. Karlsson, C. Miron, M.-N. Piancastelli, S. L. Sorensen, H. Wang, K. Wiesner, and S. Svensson, Phys. Rev. A **65**, 034705 (2002).
[46] A. Machado Bueno, A. Naves de Brito, R. F. Fink, M. Bassler, O. Bjorneholm, F. Burmeister, R. Feifel, C. Miron, S. L. Sorensen, H. Wang, and S. Svensson, Phys. Rev. A **67**, 022714 (2003).
[47] R. F. Fink, A. Eschner, M. Magnuson, O. Björneholm, I. Hjelte, C. Miron, M. Bassler, S. Svensson, M. N. Piancastelli, and S. L. Sorensen, J. Phys. B **39**, L269 (2006).
[48] K. Faegri, Jr. and H. P. Kelly, Phys. Rev. A **19**, 1649 (1979).
[49] J. A. Richards and F. P. Larkins, J. Phys. B **17**, 1015 (1984).
[50] F. P. Larkins and J. A. Richards, Aust. J. Phys. **39**, 809 (1986).
[51] K. Zähringer, H.-D. Meyer, and L. S. Cederbaum, Phys. Rev. A **45**, 318 (1992).

[52] K. Zähringer, H.-D. Meyer, L. S. Cederbaum, F. Tarantelli, and A. Sgamellotti, Chem. Phys. Lett. **206**, 247 (1993).

[53] S. K. Botting and R. R. Lucchese, Phys. Rev. A **56**, 3666 (1997).

[54] B. Schimmelpfennig, B. M. Nestmann, and S. D. Peyerimhoff, J. Electron Spectrosc. Relat. Phenom. **74**, 173 (1995).

[55] B. Schimmelpfennig and S. D. Peyerimhoff, Chem. Phys. Lett. **253**, 377 (1996).

[56] V. Carravetta and H. Ågren, Phys. Rev. A **35**, 1022 (1987).

[57] V. Carravetta and H. Ågren, J. Phys. **48**, C9-769 (1987).

[58] H. Ågren and V. Carravetta, J. Chem. Phys. **87**, 370 (1987).

[59] V. Carravetta, H. Agren, O. Vahtras, and H. Jensen, J. Chem. Phys. **113**, 7790 (2000).

[60] D. E. Ramaker, J. S. Murday, N. H. Turner, G. Moore, M. G. Lagally, and J. Houston, Phys. Rev. B **19**, 5375 (1979).

[61] E. Ohrendorf, H. Köppel, L. S. Cederbaum, F. Tarantelli, and A. Sgamellotti, J. Chem. Phys. **91**, 1734 (1989).

[62] F. Tarantelli, A. Sgamellotti, and L. S. Cederbaum, J. Chem. Phys. **94**, 523 (1991).

[63] T. R. Walsh, T. E. Meehan, and F. P. Larkins, J. Phys. B **27**, 2211 (1994).

[64] T. R. Walsh, T. E. Meehan, and F. P. Larkins, J. Phys. B **27**, L657 (1994).

[65] M. Mitani, O. Takahashi, K. Saito, and S. Iwata, J. Electron Spectrosc. Relat. Phenom. **128**, 103 (2003).

[66] A. K. Edwards, Q. Zheng, R. M. Wood, and M. A. Mangan, Phys. Rev. A **55**, 4269 (1997).

[67] R. R. Lucchese, A. Lafosse, J. C. Brenot, P. M. Guyon, J. C. Houver, M. Lebech, G. Raseev, and D. Dowek, Phys. Rev. A **65**, 020702 (2002).

[68] V. Balashov, A. Grum-Grzhimailo, and N. Kabachnik, *Correlation and Polarization Phenomena in Atomic Collisions. A Practical Theory Course* (Plenum, New York, 2000).

[69] D. Varshalovich, A. Moskalev, and V. Khersonskii, *Quantum Theory of Angular Momentum* (World Scientific, Singapore, 1988).

[70] M. N. Piancastelli, M. Neeb, A. Kivimäki, B. Kempgens, H. M. Köppe, K. Maier, A. M. Bradshaw, and R. F. Fink, J. Phys. B **30**, 5677 (1997).

[71] K. P. Huber and G. Herzberg, *Molecular Spectra and Molecular Structure IV. Constants of Diatomic Molecules* (Van Nostrand, New York, 1979).

[72] T. H. Dunning, Jr., J. Chem. Phys. **90**, 1007 (1989).

[73] C. F. Froese Fischer, T. Brage, and P. Jönsson, *Computational Atomic Structure, An MCHF Approach* (Institute of Physics, Bristol, 1997).

[74] R. F. Fink (unpublished).

[75] M. H. Chen, F. P. Larkins, and B. Crasemann, At. Data Nucl. Data Tables **45**, 1 (1990).

[76] C.-M. Liegener, Chem. Phys. Lett. **90**, 188 (1982).

[77] R. F. Fink, "*Ab initio* calculations of molecular auger electron spectra," Habilitation thesis, University of Bochum, 2001.

[78] W. B. Westerveld, J. van der Weg, J. van Eck, H. G. M. Heideman, and J. B. West, Chem. Phys. Lett. **252**, 107 (1996).

[79] M. N. Piancastelli, R. F. Fink, R. Feifel, M. Bässler, S. L. Sorensen, C. Miron, H. Wang, I. Hjelte, O. Björneholm, A. Ausmees, S. Svensson, P. Satek, F. K. Gel'mukhanov, and H. Ågren, J. Phys. B **33**, 1819 (2000).

[80] C.-M. Liegener and R. Chen, J. Chem. Phys. **88**, 2618 (1988).

[81] T. Porwol, G. Dömötör, H.-J. Freund, R. Dudde, C.-M. Liegener, and W. von Niessen, Phys. Scr. **T41**, 197 (1992).

[82] C.-M. Liegener, J. Chem. Phys. **104**, 2940 (1996).

[83] U. Hergenhahn, A. Rüdel, K. Maier, A. M. Bradshaw, R. F. Fink, and A. T. Wen, Chem. Phys. **289**, 57 (2003).

[84] T. Porwol, G. Dömötör, I. Hemmerich, J. Klinkmann, H.-J. Freund, and C.-M. Liegener, Phys. Rev. B **49**, 10557 (1994).

[85] J. Klinkmann, D. Cappus, K. Homann, T. Risse, A. Sandell, T. Porwol, H. Freund, K. Fink, R. Fink, and V. Staemmler, J. Electron Spectrosc. Relat. Phenom. **77**, 155 (1996).